Journal of
Composites Science

MDPI

Article

Biocomposites Based on Polyethylene/Ethylene–Vinyl Acetate Copolymer/Cellulosic Fillers

P. G. Shelenkov [1], P. V. Pantyukhov [1,2,*], A. V. Krivandin [1], A. A. Popov [1,2], B. B. Khaidarov [2,3] and M. Poletto [4]

[1] Emanuel Institute of Biochemical Physics, Russian Academy of Sciences, Moscow 119334, Russia; anatoly.popov@mail.ru (A.A.P.)
[2] Higher Engineering School "New Materials and Technologies", Plekhanov Russian University of Economics, Moscow 117997, Russia
[3] Department of Functional Nanosystems and High-Temperature Materials, National University of Science & Technology (MISIS), Moscow 119049, Russia
[4] Postgraduate Program in Engineering of Processes and Technologies (PGEPROTEC), University of Caxias do Sul (UCS), Caxias do Sul 95070-560, Brazil
* Correspondence: p.pantyukhov@gmail.com

Abstract: This work studied biocomposites based on a blend of low-density polyethylene (LDPE) and the ethylene–vinyl acetate copolymer (EVA), filled with 30 wt.% of cellulosic components (microcrystalline cellulose or wood flour). The LDPE/EVA ratio varied from 0 to 100%. It was shown that the addition of EVA to LDPE increased the elasticity of biocomposites. The elongation at break for filled biocomposites increased from 9% to 317% for microcrystalline cellulose and from 9% to 120% for wood flour (with an increase in the EVA content in the matrix from 0 to 50%). The biodegradability of biocomposites was assessed both in laboratory conditions and in open landfill conditions. The EVA content in the matrix also affects the rate of the biodegradation of biocomposites, with an increase in the proportion of the copolymer in the polymer matrix corresponding to increased rates of biodegradation. Biodegradation was confirmed gravimetrically by weight loss, an X-ray diffraction analysis, and the change in color of the samples after exposition in soil media. The prepared biocomposites have a high potential for implementation due to the optimal combination of consumer properties.

Keywords: biocomposite; highly filled biocomposite; masterbatch; ethylene–vinyl acetate copolymer (EVA); low-density polyethylene (LDPE); wood flour; microcrystalline cellulose; mechanical properties; phase structure; biodegradation; X-ray diffraction analysis; scanning electron microscopy (SEM)

Citation: Shelenkov, P.G.; Pantyukhov, P.V.; Krivandin, A.V.; Popov, A.A.; Khaidarov, B.B.; Poletto, M. Biocomposites Based on Polyethylene/Ethylene–Vinyl Acetate Copolymer/Cellulosic Fillers. *J. Compos. Sci.* **2024**, *8*, 464. https://doi.org/10.3390/jcs8110464

Received: 11 September 2024
Revised: 3 November 2024
Accepted: 5 November 2024
Published: 8 November 2024

1. Introduction

Plastic waste, being non-degradable in the environment, has become one of the most urgent problems in recent decades. The period of the full biodegradation of polyethylene is estimated as more than 100 years [1,2]. One of the ways to solve this problem is the preparation of biodegradable packaging materials with a short lifecycle. There is a large number of biodegradable plastics in the world. At the same time, they can be used in various areas of human life, from simple packaging to the transport of drugs [3,4], as well as materials for implants [5,6]. However, not all of the so-called "biodegradable" goods available to buy in supermarkets are biodegradable in soil media [7,8]. The idea of preparing biocomposite materials for goods with short lifecycles looks promising. Biocomposites may be made of a biodegradable polymer matrix or biodegradable filler, or both the matrix and the filler should be biodegradable [9]. Polysaccharide fillers, like cellulose, starch, dextrin, chitosan, and food production wastes, are most commonly used for the preparation of biocomposites [3,10,11]. The biocomposites created in this work can be used as packaging materials, bags, and containers for various types of goods. The advantages of such biocomposites

compared to polymers that consist entirely of natural raw materials, such as polylactide, for example, are their low cost and high-performance characteristics. The estimated period of the full biodegradation of these biocomposites is 5–15 years [12,13], and the biodegradation of pure synthetic polymers may take hundreds of years [14]. It is possible to accelerate the biodegradation of polyethylene by the addition of both the biodegradable filler [15] and the oxidative degradation initiator ("oxo-additive") [16,17]. The introduction of oxo-additives to polyolefins accelerates the process of oxidative degradation, at first reducing the molecular weight of the polymer and then promoting the destruction of low-molecular-weight fragments [18,19].

Wood flour (finely ground wood shavings) is often used as a filler for biocomposites [20–22]. It has widespread availability and low cost (USD 0.1–0.3 per kg). In work [23], it was found that biocomposites with wood flour are more stable in response to thermo-oxidative destruction. That effect was explained by the diffusion of low-molecular-weight polyphenols from wood flour into a polymer matrix. It significantly expands the possibilities for recycling and increases the number of recycling cycles.

The rate of biodegradation depends on the nature of the biocomposites' components, their adhesion, and the conditions of the environment [24]. The crystallinity degree is the other key factor influencing biodegradability. Macromolecules are packed less tightly in amorphous regions; that is why these regions are more prone to biodegradation and the crystalline parts are more stable against biodegradation. The mobility of the macromolecular segments in the composite is also important for biodegradation. The weight loss of the composite increases with increasing mobility of macromolecular segments. The main problem in the preparation of such materials is the poor compatibility of the polar (hydrophilic) filler and the non-polar (hydrophobic) polymer matrix. The introduction of compatible additives, so-called compatibilizers, may improve the performance properties of biocomposites. Typically, compatibilizers contain polar and non-polar parts. The most commonly used compatibilizers are based on maleic anhydride [25–27]. One of the alternative compatibilizers is the ethylene–vinyl acetate copolymer (EVA) since it has both polar and non-polar units. It was shown by Li et al. (2012) [28] that the addition of EVA into a composite, made of polyethylene and wood flour, enhanced the interaction between the polyethylene and the filler. In the work devoted to LDPE by Pham (2021) [29], the issue of using EVA as a compatibilizer was also considered. The author notes that a material based on recycled polyethylene with the addition of EVA and wood flour may be an effective solution to the issue of minimizing plastic waste. The addition of EVA into PE-based composite materials improves their mechanical properties. The highest elongation at break was found in the composite based on recycled polyethylene with the addition of 10 wt.% EVA.

Highly filled biocomposites, based on five different grades of EVA and containing 50–70 wt.% of the filler, were studied in previous works [30–32]. The EVA grader differed by the melt flow index (MFI) and vinyl acetate content. Mechanical and rheological properties of highly filled biocomposites, based on EVA and wood flour, were studied [30]. In another work by Shelenkov et al. (2020) [31], the results of masterbatches, filled with microcrystalline cellulose, were published. The properties of highly filled biocomposites based on EVA, including an analysis of the fractional composition, a thermogravimetric analysis of fillers, water absorption, scanning electron microscopy, optical microscopy, and mechanical and rheological characteristics, were presented [32]. It was found that the optimal combination of mechanical and rheological properties contained a biocomposite based on EVA with MFI = 25 g/10 min and 28 wt.% of vinyl acetate (LG Chem EA28025, Seoul, Republic of Korea).

This article presents a continuation of this series of works. The final biocomposites, made of masterbatches, based on LG Chem EA28025, were investigated. The obtained biocomposites may be used for the production of disposable products and packaging materials. To obtain such final biocomposites, the masterbatches based on EVA were mixed with LDPE, with different ratios of EVA to LDPE and the same filler content (30 wt.%). The work aimed to determine the optimal ratio of EVA/LDPE in the biocomposite, and to select

the optimal filler. Usually, the combination of highly desired consumer properties, high biodegradability, and the ease of industrial processing cannot be found in one material, but the combination of sufficient properties is possible to find in several compositions. It is more important to study the phase structure to find correlations between composition and mechanical and rheological properties and biodegradability.

2. Materials and Methods

2.1. Materials

For the preparation of biocomposites, LDPE made by UfaOrgSyntez (Ufa, Russia), grade 10803-020, and EVA made by LG Chem (Seoul, Republic of Korea), grade EA 28025, were used. The basic characteristics of the polymers are presented in Table 1. Microcrystalline cellulose (MCC) made by LLC Progress (Kemerovo, Russia), grade 101, and wood flour (WF), which is a mixture of coniferous and deciduous trees, supplied by LLC Novotop (Moscow region, Russia), grade 140, were used as fillers. Table 2 shows the chemical composition of the fillers used. The fillers were sifted through a sieve with a mesh size of 100 μm; photographs of the initial fillers are shown in Figure 1.

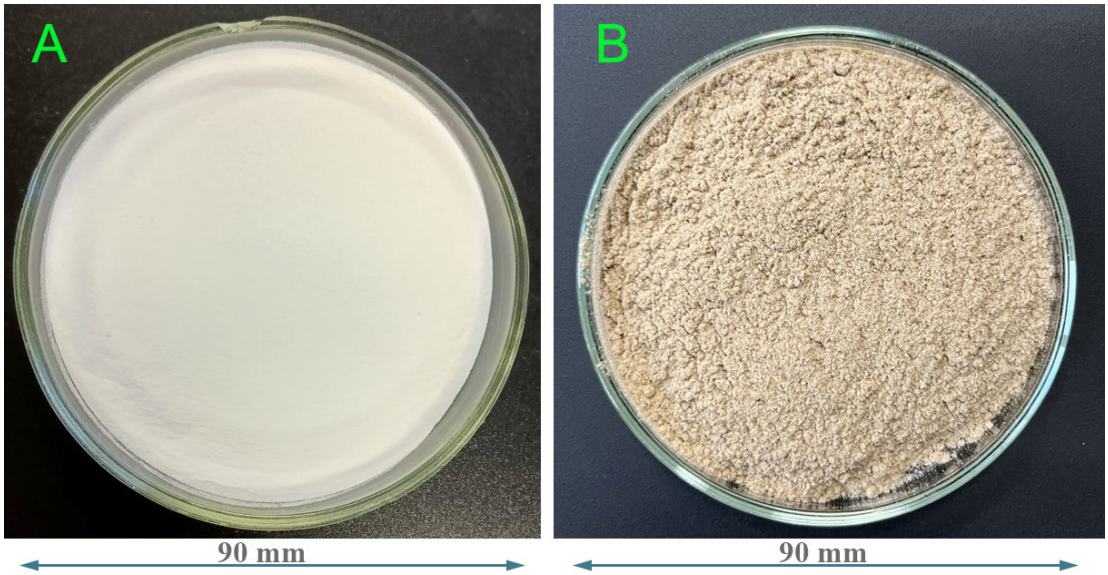

Figure 1. Photographs of the fillers: (**A**)—microcrystalline cellulose (MCC), (**B**)—wood flour (WF).

Table 1. Basic characteristics of LDPE and EVA (information from manufacturers' technical data sheets).

No.	Polymer	Vinyl Acetate Content		Melt Flow Index (MFI) [g/10 min]	Tensile Strength [MPa]	Elongation at Break [%]	Density [g/cm^3]	Melting Temperature [°C]
		[wt.%]	[mol. %]					
1	Ethylene–vinyl acetate copolymer (EVA)	28	11	25	19.7	820	0.951	69
2	Low-density polyethylene (LDPE)	-	-	1.9	17.0	598	0.917	107

Table 2. Chemical composition of fillers.

Filler	Cellulose [%]	Lignin [%]	Pentosans [%]	Polyuronic Acids [%]	Reference
Wood flour (WF)	46	20	29	5	[33]
Microcrystalline cellulose (MCC)	100	-	-	-	-

The initial fillers differed by the crystallinity of the cellulose. Table 3 presents the data of an FTIR analysis and total crystalline index (TCI) of the fillers. The difference in TCI of fillers shows that MCC has a higher degree of crystallinity (approximately at 35%) than WF.

Table 3. Total crystallinity index (TCI) of fillers.

Filler	A_1372 cm^{-1}	A_2900 cm^{-1}	Total Crystalline Index (TCI)
Wood flour (WF)	0.002831	0.00229	1.2362
Microcrystalline cellulose (MCC)	0.003845	0.002014	1.909

2.2. Preparation of Samples

Triple biocomposites, consisting of LDPE, EVA, and cellulosic filler, were prepared in two stages. At the first stage, highly filled biocomposites based on EVA and cellulosic filler (MCC or WF) were prepared; the content of the filler was 50, 60, or 70 wt.%. For the optimal compounding of the components in the melt condition, heated mixing rolls, UBL6175BL (Dongguan, China), were used. The temperature of the front and rear rolls was 130 °C and 150 °C, respectively; the rotation speed was 8 rpm; and the full time of mixing was 8 min. The obtained masterbatch was crushed using a knife mill Vibrotechnik RM-120 (St. Petersburg, Russia). In the second stage, the obtained masterbatches were mixed with LDPE (at the same mixing rolls under the same conditions) in such a proportion that the filler content in each biocomposite was 30% of the full mass. Thus, the triple biocomposites (LDPE/EVA/cellulosic filler) were obtained, in which the mass content of the filler was the same, but the ratio of LDPE/EVA was different: biocomposites W13, W20, W30, and W35 and C13, C20, C30, and C35. The letter "W" means wood flour, the letter "C" means microcrystalline cellulose, and the digits following the letter refer to the EVA content in the biocomposites (Table 4). This technology of preparation biocomposites from masterbatches duplicates the technology for manufacturing materials from polymer masterbatches, proposed for implementation at industrial enterprises producing finished goods and packaging.

Using the same technological regime, but in one mixing stage, double biocomposites C0, C70, W0, and W70 (Table 4) were prepared. Additionally, we prepared a series of LDPE/EVA blends with EVA content of 0, 20, 30, 40, 50, 60, 80, 90, and 100% by weight.

Table 4. Composition of biocomposites.

Biocomposites with WF		Biocomposites with MCC	
W0	WF 30 wt.% + LDPE 70 wt.%	C0	MCC 30 wt.% + LDPE 70 wt.%
W13	WF 30 wt.% + EVA 13 wt.% + LDPE 57 wt.%	C13	MCC 30 wt.% + EVA 13 wt.% + LDPE 57 wt.%
W20	WF 30 wt.% + EVA 20 wt.% + LDPE 50 wt.%	C20	MCC 30 wt.% + EVA 20 wt.% + LDPE 50 wt.%
W30	WF 30 wt.% + EVA 30 wt.% + LDPE 40 wt.%	C30	MCC 30 wt.% + EVA 30 wt.% + LDPE 40 wt.%
W35	WF 30 wt.% + EVA 35 wt.% + LDPE 35 wt.%	C35	MCC 30 wt.% + EVA 35 wt.% + LDPE 35 wt.%
W70	WF 30 wt.% + EVA 70 wt.%	C70	MCC 30 wt.% + EVA 70 wt.%

The obtained pieces of triple biocomposites were crushed using a knife mill Vibrotechnik RM-120 (St. Petersburg, Russia). The crushed material was molded in a hydraulic press Gotech GT-7014-H (Taichung City, Taiwan) at a temperature of 140 °C in the metal frame with a thickness of 0.55 mm. As a result, sheets with a thickness of 0.5–0.6 mm were obtained for further study of mechanical properties and water absorption. For the study of weight loss during exposure in soil and X-ray diffraction studies, films with a thickness of ~250 μm were also molded in an aluminum foil frame. Cooling for all samples occurred in air at room temperature (23 ± 2 °C) for 2 min.

2.3. Research Methods

Scanning electron microscopy (SEM) was employed to capture images of the fillers (WF and MCC) and determine their particle shapes. The research utilized a Tescan Vega 3SB (Brno-Kohoutovice, Czech Republic), a fully automated SEM equipped with a conventional tungsten thermal cathode, designed for high-vacuum investigations. To examine dispersed materials and biocomposite films, samples were secured on the microscope stage using double-sided carbon conductive tape. One side of the tape was attached to the microscope's object stage, while the sample was spread as a thin layer on the opposite side. Prior to the analysis, the samples were coated with platinum. The SEM was operated under the following conditions: a 20 kV accelerating voltage, low current intensity, and 15 mm working distance.

The particles' size was determined via a Fritsch Analysette 22 laser instrument (Idar-Oberstein, Germany) in water media under the influence of ultrasound following ISO 13320.

The difference in the crystallinity of the fillers was estimated using FTIR spectroscopy. Studies were carried out using an FT-803 Simex IR-Fourier spectrometer (Novosibirsk, Russia). The IR spectra of the fillers were recorded using the ATR method on a germanium crystal with 64 scans in the range from 4000 cm^{-1} to 450 cm^{-1}. The total crystalline index (TCI) was calculated based on the intensity ratio of the absorption bands at 1372 and 2900 cm^{-1} using the method previously described [34].

A universal testing machine Gotech AI-7000M (Taichung City, Taiwan) equipped with an extensometer was utilized to assess the mechanical properties. Crosshead velocity was 100 mm/min, and the shape and size of the samples corresponded to type 5A [35]. Samples were cut out from the plates using an auto-pneumatic cutter press Gotech GT 7016 AR (Taichung City, Taiwan). At least five measurements were carried out for each composition.

The study of water absorption was conducted in accordance with standard [36]. Initially, specimens were dehydrated in an oven at 50 °C for 24 h and subsequently weighed with a precision of ±0.1 mg. The samples were then submerged in distilled water at an ambient temperature (23 ± 2 °C). At predetermined intervals, the specimens were extracted from the water, and excess moisture on their surfaces was removed using filter paper. The samples were weighed again, and the water absorption was calculated as a percentage based on the difference in weight.

Exposure of samples in combined soil occurred for the complex assessment of biodegradability. The soil was made of sand, garden soil, and horse manure taken in equal amounts (according to the standard [37]). The combined soil was held for 2 months at 20 ± 5 °C with daily stirring and humidity maintained at 60 ± 5%. The soil was placed in a plastic container at a layer thickness of 25 ± 5 cm. The samples were placed vertically in the soil; the distance between the samples was not less than 20 mm. The samples were completely hidden under the soil. The biodegradation of samples was assessed by the loss of sample weight after exposure to soil. To carry out this, after being removed from the soil, the samples were kept in air at room temperature for 3–5 days until the mass stabilized.

The supramolecular structure of the samples was studied by X-ray diffraction. The diffraction patterns were obtained in reflection using the Bragg–Brentano X-ray optical scheme on an HZG4 Freiberger Prazisionsmechanik diffractometer (Freiberg, Germany) with a graphite monochromator of diffracted radiation (CuKα radiation). The content of non-degraded filler (filler with the original structure) in biocomposite films after exposure in the soil was estimated by approximating the diffraction patterns of the films by the sum of the diffraction patterns of the components (LDPE, EVA, MCC, WF).

The color change in the samples before and after exposure to the soil was recorded via an X-Rite VS450 spectrophotometer (Grand Rapids, Michigan, USA) in the spectral range of 400–700 nm using an aperture of 6 mm under a standard D65 illuminator (daylight) with a measurement angle of 10°. The color coordinates L*a*b*C*h were measured.

The research was conducted utilizing scientific instruments from the Center of Shared Usage "New Materials and Technologies of Emanuel Institute of Biochemical Physics" and the Joint Research Center at the Plekhanov Russian University of Economics.

3. Results

Using scanning electron microscopy (SEM), it was revealed that WF particles had a more irregular shape and more branched structure than MCC particles (Figure 2). The surface of WF particles shows the delamination of fibers, while the surface of cellulose particles appears more even and smooth. Therefore, the surface area of WF particles is much higher than that of MCC at the same particle size.

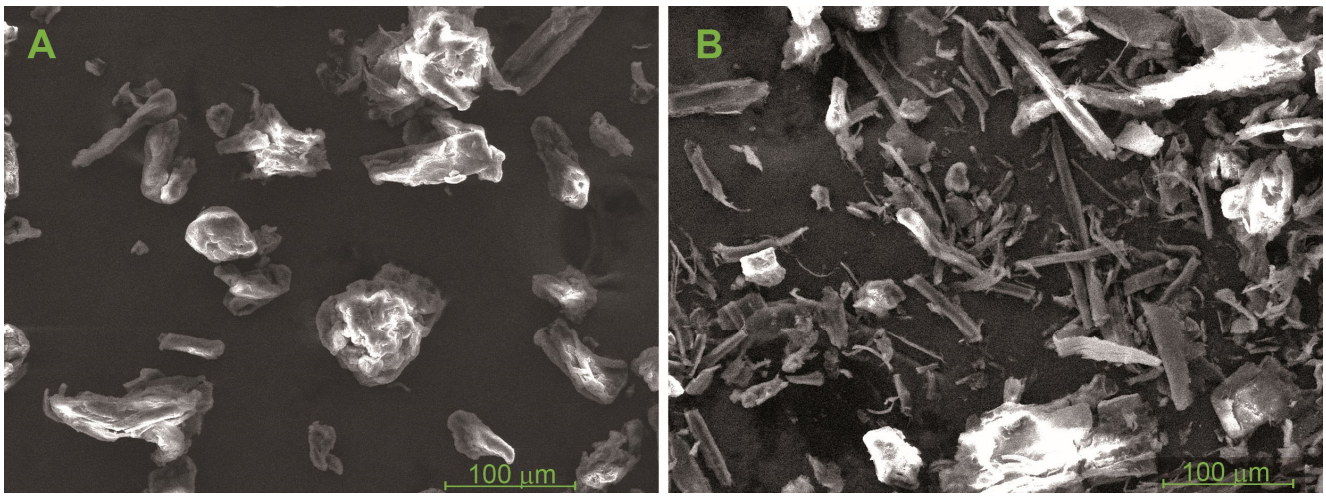

Figure 2. Photomicrographs of the fillers' particles, made by scanning electron microscopy (SEM). (**A**)—microcrystalline cellulose (MCC), (**B**)—wood flour (WF).

By using the laser diffraction method, it was found that WF had a wide range of particle size distribution (Table 5). WF particles, unlike MCC ones, have larger particles (>100 µm). It can be explained as follows: WF particles have a more elongated shape than MCC particles, which allows cylindrical WF particles, longer than 100 µm (but with a diameter less than 100 µm), to pass through the sieve mesh.

Table 5. Distribution of fillers' particles by size.

Size [µm]	Content [%]	
	MCC	WF
0–1	0.9	0.5
1–2	1.7	1.5
2–5	2.8	2.8
5–10	3.1	3.4
10–20	9.3	10.0
20–45	37.9	27.1
45–75	37.7	26.0
75–100	6.4	12.8
100–200	0.2	15.4
200–300	0	0.5

For the assessment of the mechanical characteristics of both filled and unfilled materials, we plotted the dependencies of tensile strength, elongation at break, and yield strength on the EVA content in the polymer matrix. The content of EVA in triple biocomposites is indicated on the abscissa axis (Figure 3) without taking into account the filler, so it is not EVA content in a full biocomposite per se (indicated in Table 4) but EVA content in the polymer matrix of a biocomposite. Figure 3A shows that the addition of 30 wt.% cellulosic filler to LDPE leads to a decrease in tensile strength by two times and the elongation at

break drops by an order of magnitude, from 600% to 44%, for MCC-based biocomposites and falls to 9% for WF-based ones (Figure 3B). Equal results were obtained in previous work [38]: the addition of 30 wt.% WF into an ethylene–octene copolymer matrix led to a 20% decrease in tensile strength, and elongation at break decreased by seven times. Hard filler particles do not allow macromolecules to straighten when stretched; the higher the filler content in the biocomposite, the more rigid its structure.

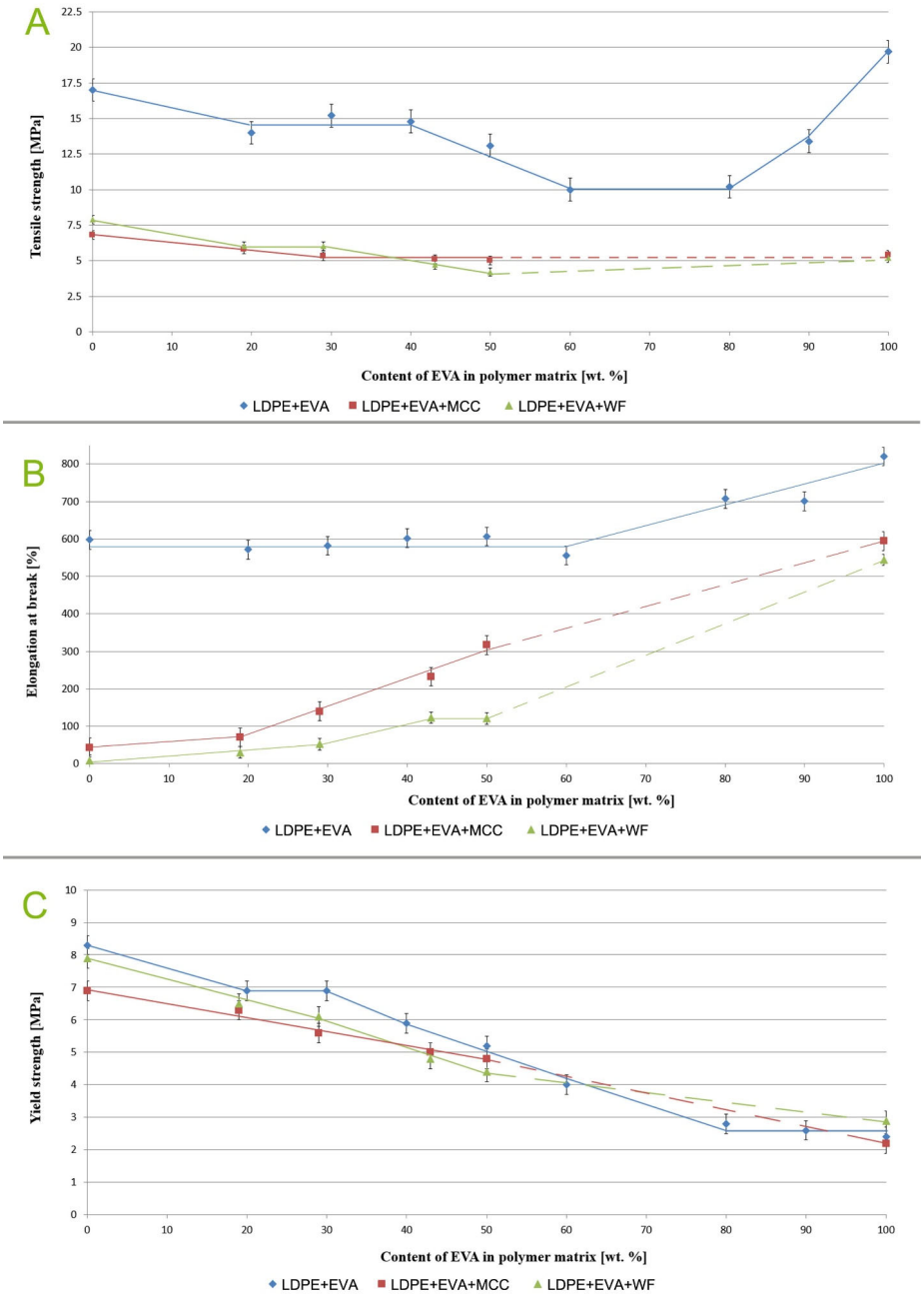

Figure 3. The dependence of mechanical characteristics [(**A**)—tensile strength, (**B**)—elongation at break, (**C**)—yield strength] on the EVA content in the polymer matrix.

The addition of 50 wt.% EVA enhances the elasticity of biocomposites; thus, elongation at break increases up to 317% for MMC-based biocomposites and to 120% for WF-based biocomposites. EVA has better adhesion to the fillers' particles than LDPE because of the chemical affinity of cellulose with the vinyl acetate group. EVA also has lower melt viscosity (the MFI of EVA is 10 times higher than that of LDPE), which is why the fillers' particles have better wettability in an EVA melt than in an LDPE melt. As a result, a less

defective structure is formed in the EVA-based biocomposite than that in LDPE (fewer air cavities inside).

Based on these data, it could be concluded that the EVA matrix is a better option for the preparation of biocomposites than LDPE. However, with an increase in the proportion of EVA, the yield strength decreases linearly. Moreover, the added filler does not affect the yield strength; this parameter is determined by the matrix only. It can be seen that the matrix made of pure EVA has an extremely low yield strength. This characteristic is the most important for assessing consumer properties since when using products made of polymeric materials, extreme stretching to the point of irreversible deformation is rare. Thus, triple biocomposites that combine the advantages of both polymer matrices have the best combination of consumer characteristics.

It is interesting to note that in polymer blends, made of LDPE and EVA, the tensile strength decreases from 0 to an EVA content of 60 wt.%, and from 80 wt.%, it begins to increase (Figure 3A). In the EVA content range of 60–80%, phase inversion is observed. EVA begins to form a polymer matrix where LDPE is distributed in the form of local inclusions.

The role of aqueous solutions penetrating deep into the sample is very important for biodegradation. Along with water, microorganisms capable of destroying the organic filler can also penetrate the sample. The kinetic curves of the water absorption of biocomposites are shown in Figure 4. The water absorption of biocomposites filled with WF or MCC increases significantly with an increase in the content of EVA in the polymer matrix from ~30 to ~40 wt.%. This can be explained by the change in the phase structure of the polymer matrix. A transition of the structure where LDPE is a dispersed medium and EVA is a dispersed phase to an interpenetrating polymer network occurs. The filler, initially encapsulated into EVA, becomes more prone to water penetration in interpenetrating polymer structures. Moreover, in MCC-based biocomposites, the curves for the composites with 0, 18.6, and 28.6% of EVA are in the same area, but in the case of WF-based biocomposites, the curves of the composites with the same EVA content separate. Phase structure has more influence on the properties of MCC-based biocomposites than on WF-based ones. Long-branched particles of WF disrupt the regularities of the polymer's phase structure. Biocomposites with WF absorb more water than the ones with MCC. This may be caused by both the looser structure of WF particles and the greater number of defects due to the rough surface of WF particles and their greater length (Figure 2 and Table 5). A similar pattern was previously found in highly filled biocomposites based on EVA with WF and MCC [26].

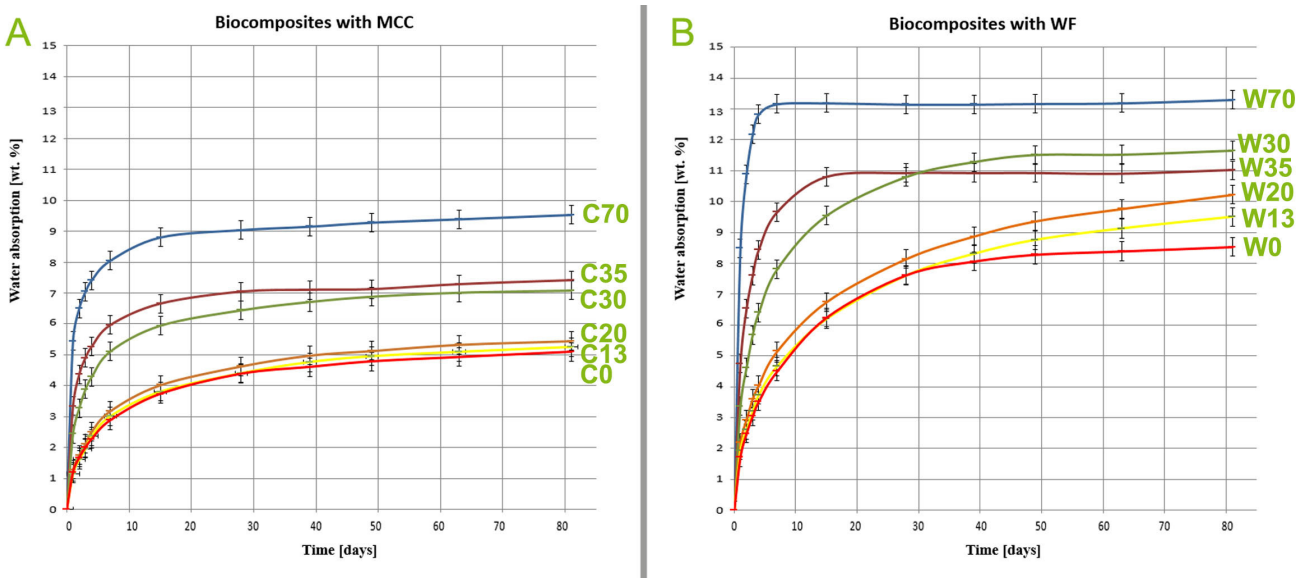

Figure 4. Biocomposites' water absorption dependence on time. [(**A**)—MCC-based biocomposites, (**B**)—WF-based biocomposites].

The results obtained on the water absorption of biocomposites were confirmed by the results of weight loss in laboratory soil and in soil in the landfill (Figure 5). The regularities in weight loss of biocomposites in laboratory conditions and at the landfill are very similar, which indicates the high reliability of the obtained results.

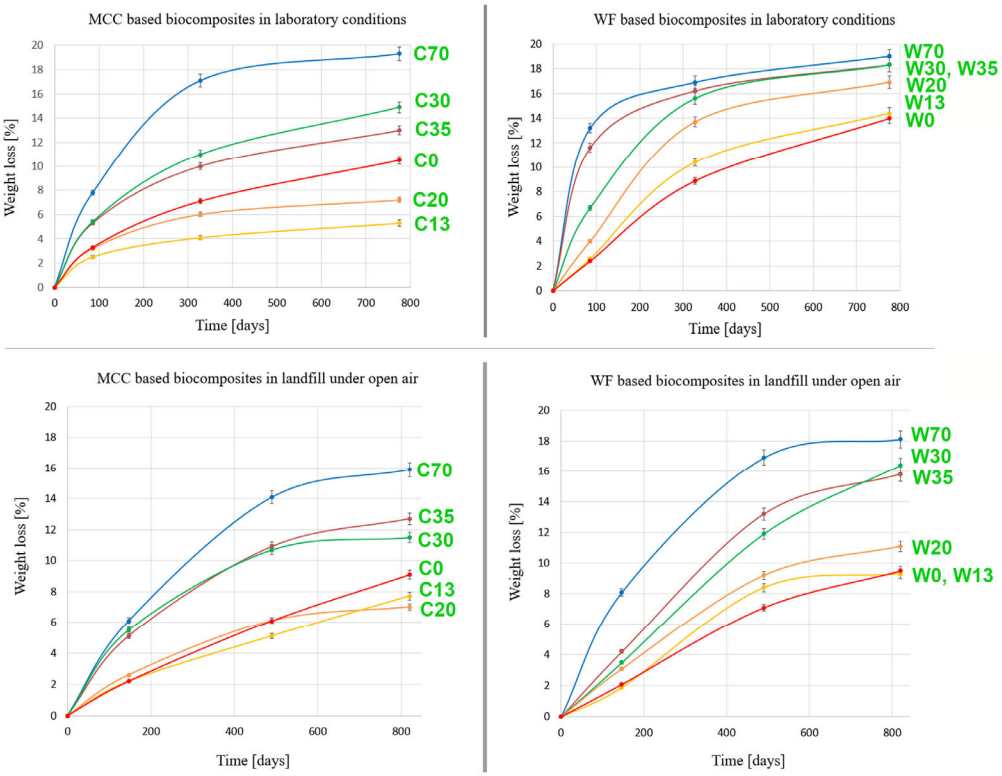

Figure 5. Dependence of biocomposites' weight loss, in laboratory conditions and in landfill under open air, on EVA content in polymer matrix.

WF-based biocomposites had higher weight loss than MCC-based ones. It can be explained by the shape of the WF particles: they are elongated and may form a net that works as a transport system for water solutions. Besides this, because of the high crystallinity degree of MCC, its biodegradability is lower than that of WF [39].

With an increase in EVA content in the polymer matrix, a tendency towards an increase in the weight loss of biocomposites is observed, clearly expressed in all experiments with a change in EVA content in the polymer matrix from ~30 to ~40% (Figure 5). As in the case of water absorption, this also confirms that with an increase in EVA content in the polymer matrix from ~30 to ~40%, the matrix rearranges to a mutually penetrating structure of two polymers (EVA and LDPE). The entire volume of the biocomposite becomes accessible to the influence of the external aqueous environment that contains microorganisms capable of destroying the organic filler.

In triple biocomposites with MCC, at EVA contents of 18.6% and 28.6% in the polymer matrix, the weight loss was significantly lower than in double biocomposites made of LDPE and MCC. At low concentrations (up to 30 wt.%), EVA exists as a dispersed phase into LDPE. Most MCC particles are encapsulated in EVA, which is encapsulated into an LDPE matrix. For that reason, MCC particles are isolated from an external water medium and microorganisms. In the same biocomposites with WF, that tendency does not exist. Long WF particles cannot be encapsulated by EVA inclusions; the particles have contact with each other, forming a net that promotes the penetration of external media inside the biocomposite.

To analyze the changes in the structure of biocomposites during biodegradation, a comparative X-ray diffraction study was conducted. Biocomposite films after exposure

to laboratory soil for 775 days and control films of the same composition stored in laboratory conditions without contact with soil were studied. The structure of individual components of these biocomposites (LDPE and EVA films, MCC and WF powders) was preliminarily studied. The diffraction patterns of LDPE, EVA, MCC, and WF are shown in Figure 6A. LDPE film has an amorphous–crystalline structure with a rhombic crystal lattice, a crystallinity degree of 35%, and an average crystallite size of 15 nm (the calculation was carried out using the Selyakov–Scherrer formula based on the width of the main diffraction maximum of PE at $2\theta \approx 21.4^\circ$). At the same time, EVA film has a predominantly amorphous structure with a very small content of the crystalline phase (5%). The diffraction patterns of MCC and WF powders contain broad (diffuse) diffraction maxima (Figure 6A). MCC, as expected, consists mainly of very small crystallites (Figure 6A). The diffuse maxima on the WF diffraction pattern are even wider than on the MCC diffraction pattern, but in terms of the ratio of their intensities and position, they correspond to the diffuse maxima on the MCC diffraction pattern. The main contribution to the diffraction pattern of WF is made by cellulose, which has an amorphous structure and/or contains even smaller and less ordered crystallites than MCC crystallites.

The diffraction patterns of the C0 (designation of samples are presented in Table 4) film in the initial state and after exposure in laboratory soil for 775 days are almost identical (Figure 6B). Only a slight decrease in intensity is observed near the angle $2\theta \approx 22.5^\circ$, corresponding to the position of the most intense diffraction peak of MCC. It may be explained by a slight reduction in MCC content in the sample after exposition in soil. The structure of LDPE did not change. The results of the X-ray diffraction analysis of C0 films after 775 days of exposure in laboratory soil and in landfill soil were the same. The analysis of diffraction patterns showed that in C0 films, the content of MCC after exposure to soil was reduced by 25%. Considering that the initial MCC content in the film was 30%, we found that the weight loss of film C0 during exposure to soil should not exceed 8% (Table 6). This value is significantly less than 10.5%, obtained as a result of direct measurements of the weight loss of the films (Figure 5).

The diffraction patterns of C20 and C70 films, exposed for 775 days in soil, differed significantly from the diffraction patterns of initial films of the same composition (Figure 6C,D). The different diffraction patterns, obtained by subtracting the diffraction patterns of the films exposed in the soil from the ones of the control films, are also presented in Figure 6C,D. They contain diffraction peaks at $2\theta \approx 15.5^\circ$ and $2\theta \approx 22.5^\circ$, which are characteristic of MCC (the narrow diffraction peak of low intensity at $2\theta \approx 18^\circ$, which is not characteristic of the components of these films, presented in Figure 6C, is apparently caused by a small amount of an unidentified crystalline impurity). Consequently, the diffraction patterns of C20 and C70 films exposed in soil differ from the diffraction patterns of the initial films by a significant decrease in the contribution of the diffraction intensity of MCC. When the C20 and C70 films were exposed to soil, the biodegradation of MCC occurred, and the structure of the PE and EVA, remaining in the films, did not change noticeably. The analysis of diffraction patterns showed that in the C20 and C70 films after exposure to soil, 18% and 10% of undegraded MCC, respectively, remained. If all degraded MCC had been washed out of the films, then this would have led to a decrease in the weight of C20 and C70 films by 12% and 20%, respectively (Table 6). However, the filler weight loss value for C70 was 19.3%, while for C20, a slightly lower value of 7.2% was obtained (Figure 5). When C20 film was exposed to soil, not all of the degraded MCC was likely washed out of it. Also, an increase in the weight of the sample can be caused by its biological overgrowth with soil fungi and bacteria. Thus, the data of the X-ray diffraction analysis of biocomposites with MCC allow us to conclude that in triple biocomposites (containing EVA in polymer matrix), in contrast to double biocomposites (based on LDPE without EVA), the biodegradation of MCC is noticeably more intense.

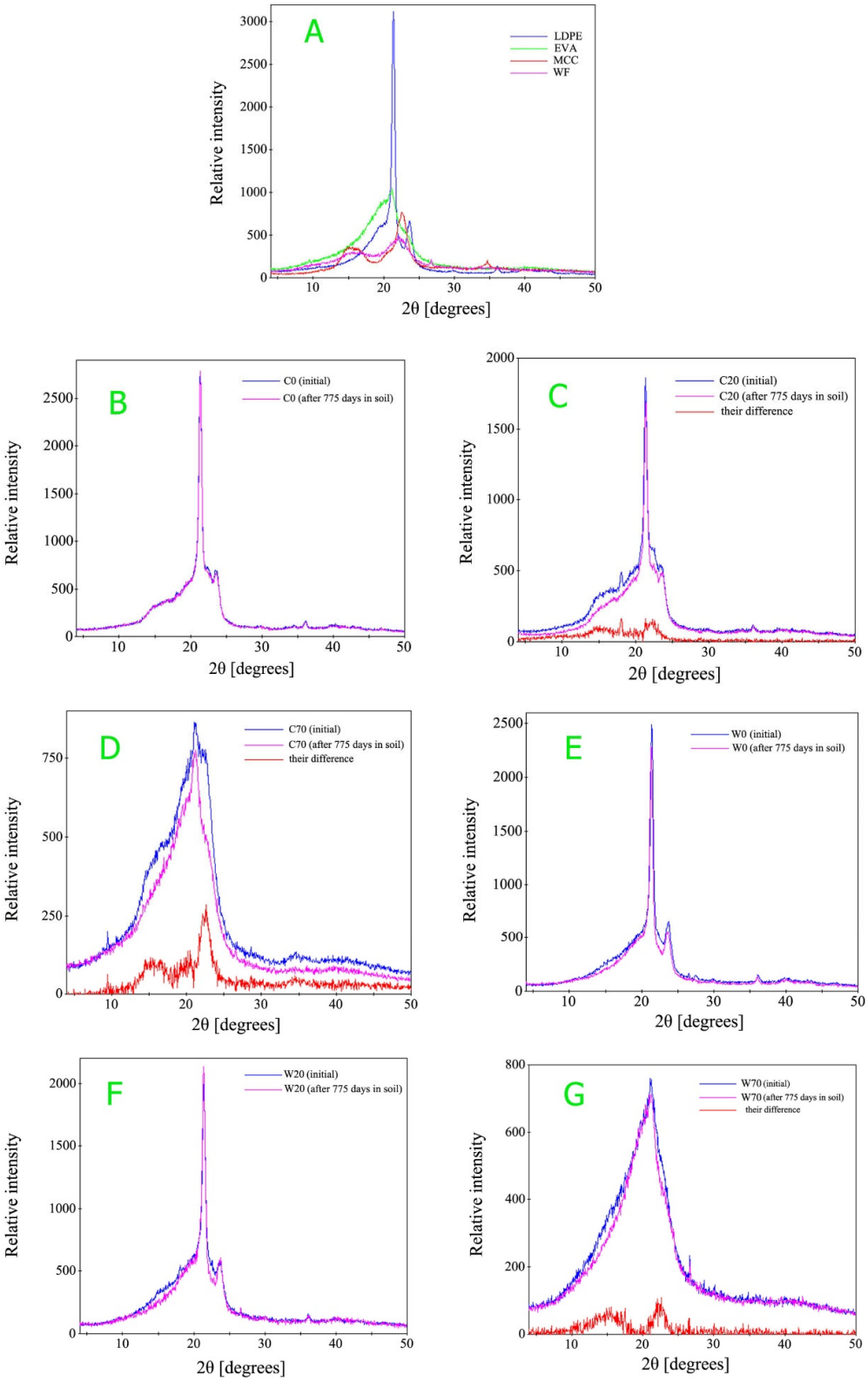

Figure 6. Diffraction patterns of LDPE, EVA, MCC, and WF (**A**); C0 (**B**); C20 (**C**); C70 (**D**); W0 (**E**); W20 (**F**); W70 (**G**).

Table 6. Amount of degraded filler was determined by X-ray diffraction method and by weighing.

Sample	EVA Content in Polymer Matrix [wt.%]	Content of Destructed Filler in Laboratory Soil [wt.%] (X-Ray Diffraction)	Weight Loss in Laboratory Soil [wt.%] (Weighing Method)	Weight Loss in Landfill Soil [wt.%] (Weighing Method)
C0	0	<8	10	9
C20	28.6	12	7	7
C70	100	20	19	16
W0	0	11	14	10
W20	28.6	18	17	11
W70	100	20	19	18

The same tendency of accelerating the biodegradation of the filler with an increase in the content of EVA in the biocomposite was observed according to X-ray diffraction data for biocomposites filled with WF (Figure 6E–G and Table 6). When assessing the content of non-degraded WF in samples W0, W20, and W70 using the X-ray diffraction method, the results we obtained were comparable results to the values obtained by the direct weighing of samples (Table 6 and Figure 5).

In double biocomposites (based on LDPE without EVA), after exposure to soil in the case of WF, significantly less undegraded filler remained (19% in D0) than in the case of MCC (>25% in C0). This is explained by the low biodegradability of MCC, as shown in previous work [39].

At the same time, the content of non-degraded MCC and WF in double biocomposites based on EVA (samples C70 and D70), according to X-ray diffraction data, was the same (Table 6). It can be assumed that part of the filler (1/3) became encapsulated in the EVA matrix and was inaccessible to the penetration of the external environment.

It can be concluded that with an increase in EVA content, the loss of filler also increases, as evidenced by the difference in the diffraction patterns of the samples before and after exposure to the soil. This conclusion was confirmed by two methods: the X-ray diffraction method and gravimetrically (the method of direct weighing).

With an increase in EVA content in the biocomposite, biofouling also increases. It can be clearly seen on the surface of the samples filled with cellulose since the initial samples were white. Figure 7 demonstrates the photographs of samples with MCC, both initially and after exposure to soil under laboratory conditions for 775 days. Biocomposites with WF initially had dark coloration and spots of biofouling and were not so clearly seen in the photographs of MCC-based biocomposites. For that reason, photographs of WF-based biocomposites after exposure to soil are not included in this paper.

Biocomposites containing more than 40% EVA in the polymer matrix (C30, C35, C70) have the obvious spots of biofouling like blackening and local yellowing. It was previously noted that when moving from 30 to 40% of EVA in the matrix, a restructuring of the phase structure occurs and an interpenetrating polymer network forms. The change in the color of the samples after exposition in soil with the initial samples was recorded using a spectrophotometer in color coordinates L*a*b* (Table 7).

Significant changes in the color coordinates of the samples begin with biocomposite C30. Starting with this composition, the samples become noticeably darker (ΔL) and their color becomes more saturated (ΔC). At the EVA content of 42.9 wt.% in the polymer matrix, yellow (Figure 8A) and pink (Figure 8B) spots appear on the surface of the samples after the biodegradation test.

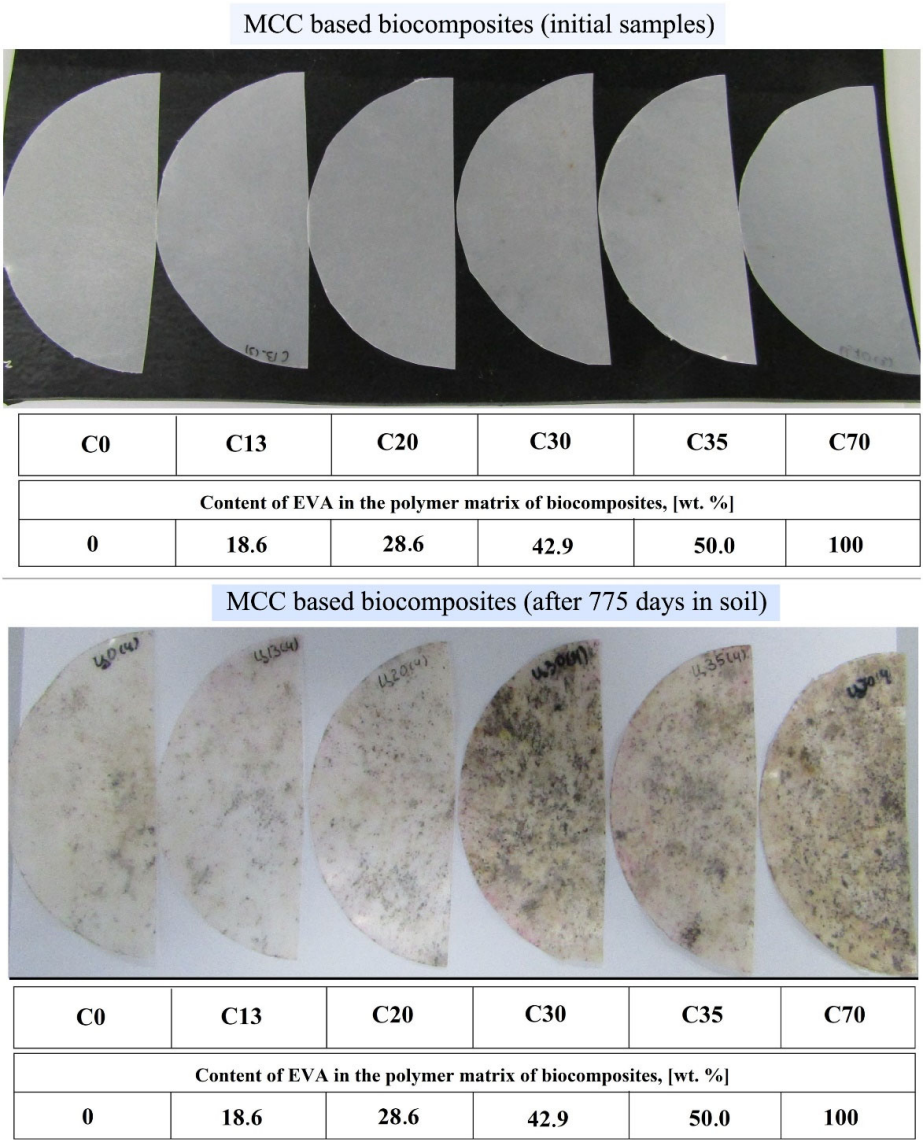

Figure 7. Photographs of the initial samples with MCC (**top row**) and photographs of the samples with MCC after 775 days of exposition in soil under laboratory conditions (**lower row**).

Table 7. Changes in color coordinates of biocomposites with MCC after exposition in soil with the initial samples.

Difference in Color Coordinates	C0	C13	C20	C30	C35	C70
ΔL*	−6.87	−5.93	−5.14	−18.76	−18.85	−23.52
Δa*	1.66	1.78	1.88	4.25	4.32	4.91
Δb*	5.37	3.12	5.98	12.4	9.63	11.2
ΔC*	4.88	2.63	5.49	12.15	9.44	11.11
Δh*	−34.6	−36.01	−36.12	−44.35	−46.96	−47.86

Note: L is the coordinate responsible for the lightness of the sample; a is the position of the color in the range from green-blue to red-crimson; b is from blue to yellow. C (chroma) is the saturation coordinate in color space. A saturation of zero indicates a completely neutral color, while a high C* value indicates a more saturated color. h (hue) is the coordinate of the hue angle in the color space, where red is 0, yellow is 90, green is 180, and blue is 270.

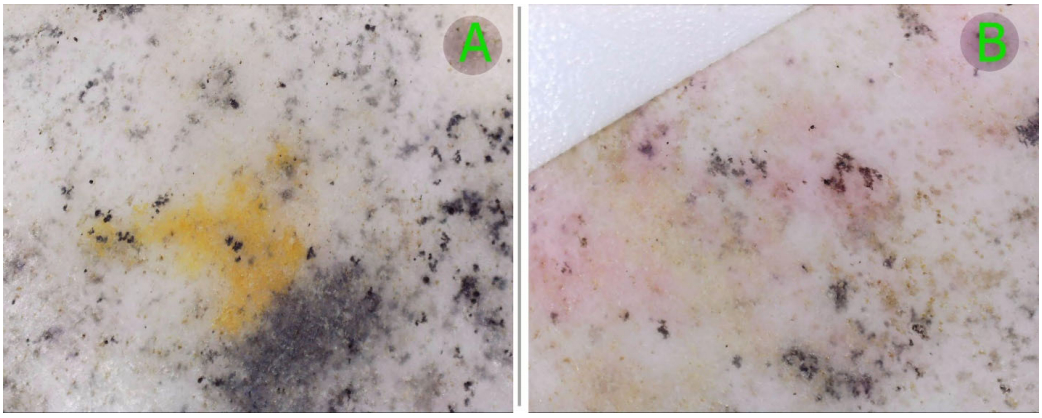

Figure 8. Traces of the impact of soil microbiota on the surface of the triple biocomposite C30. Yellowing of the film surface (**A**). Pink spot on the film surface (**B**).

Black inclusions on the surface of the samples are most likely Aspergillus niger, a pathogenic saprophytic fungus. It can destroy biocomposite materials based on polyethylene and cellulosic fillers, as shown in previous work [7]. Yellow and pink spots are most likely traces of the presence of bacteria.

The massive surface degradation of the samples was found in microphotographs, obtained by SEM. Figure 9 shows the difference between surfaces of the initial MCC-based biocomposites and the same ones after exposure in soil media. Cracks and cavities are found throughout the entire surface of the samples. These damages to the sample will further lead to its further fragmentation.

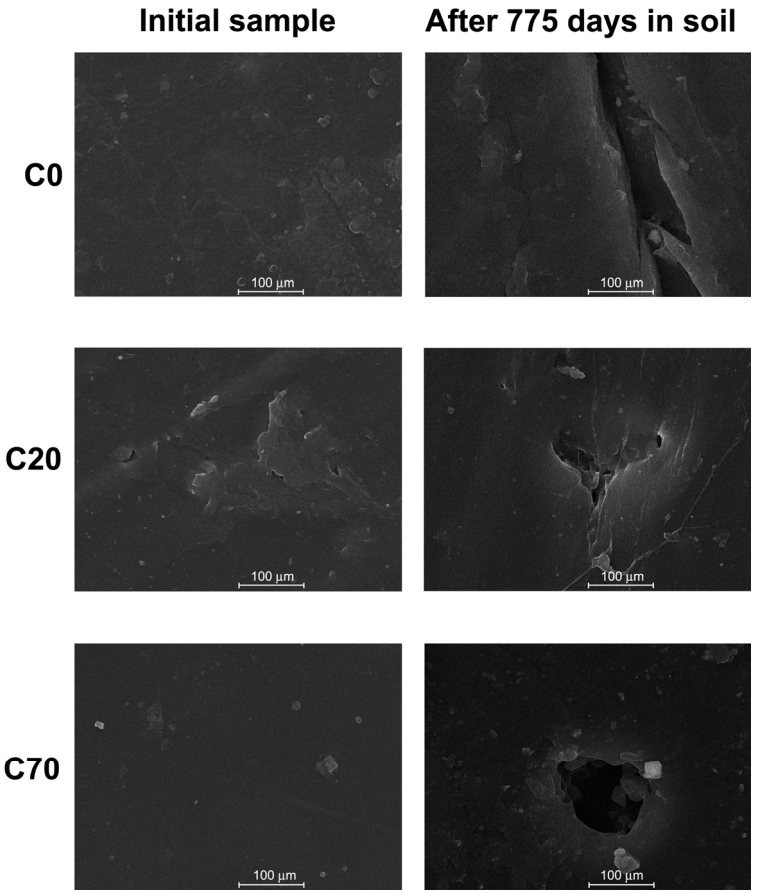

Figure 9. Microphotographs (SEM) of the surface of MCC-based biocomposites. The comparison of the initial biocomposites and after exposure to soil media samples.

More extensive damage was found on the surface of samples with WF (Figure 10). It corresponds with the data of weight loss (Figure 5); WF-based biocomposites lost more weight than MCC-based biocomposites. The biodegradation of particles with a more developed surface leads to a greater destruction of the polymer matrix. In addition, other possible explanations for the different degradation behavior observed for MCC and WF can be associated with the chemical structure of both materials [24,30,31]. As presented in Table 3, MCC has higher TCI than WF, which can contribute to lower water absorption, observed in Figure 4, due its higher ordered structure. So, it is possible that during soil sample degradation, the presence of WF can contribute to higher water absorption, which accelerates soil degradation, as observed in Figure 10, when compared to MCC.

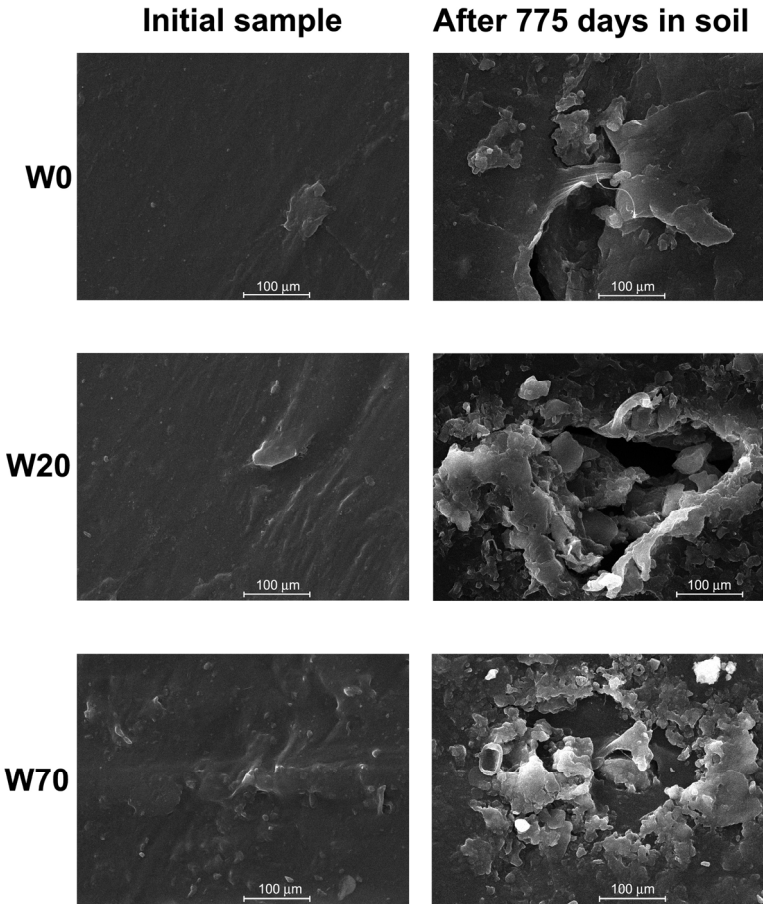

Figure 10. Microphotographs (SEM) of the surface of WF-based biocomposites. The comparison of the initial biocomposites and after exposure to soil media samples.

4. Conclusions

Physical and mechanical tests showed that at the initial deformation, characterized by the yield point, the presence of 30 wt.% filler did not affect this parameter. The tensile strength at break (at maximum deformation) was reduced by half compared to the unfilled composition over the entire range of the LDPE/EVA ratio in the polymer matrix. The elongation at break for filled biocomposites decreased by 1.5–2 orders of magnitude, increasing with an increase in the content of EVA in the polymer matrix. Elongated and highly branched WF particles reduced the elongation at break more significantly compared to the spherical and smooth MCC particles.

The content of EVA in a composition with a natural filler significantly affects the rate and degree of biodegradation; with an increase in the proportion of copolymers in the polymer matrix, the rate of biodegradation increases. It was indicated by experimental

data on the weight loss of samples after soil involvement, data from the X-ray structural analysis, visual observations, and the quantitative analysis of color change.

The phase structure of the tested biocomposites was established. Three ranges were determined: (1) LDPE is a dispersion medium with an inclusion phase of EVA (EVA content in polymer matrix of 0–30 wt.%); (2) the interpenetrating polymer structure (EVA content in polymer matrix of 40–70 wt.%); (3) EVA is a dispersion medium with an inclusion phase of LDPE (EVA content in polymer matrix of 80–100 wt.%). The effect of the encapsulation of the MCC particles by EVA inclusions was established at a low concentration of EVA in the polymer matrix (up to 30 wt.%).

Author Contributions: Conceptualization, P.G.S., P.V.P., A.V.K., A.A.P., B.B.K. and M.P.; methodology, P.G.S., P.V.P. and A.V.K.; validation, P.V.P., A.V.K., A.A.P., B.B.K. and M.P.; formal analysis, P.G.S., P.V.P. and A.V.K.; investigation, P.G.S. and P.V.P.; resources, P.V.P., A.V.K., A.A.P. and B.B.K.; data curation, P.G.S.; writing—original draft preparation, P.G.S., P.V.P. and A.V.K.; writing—review and editing, A.A.P., B.B.K. and M.P.; visualization, P.G.S.; supervision, P.V.P.; project administration, P.V.P. All authors have read and agreed to the published version of the manuscript.

Funding: This research received no external funding.

Data Availability Statement: The article contains all relevant data.

Acknowledgments: Poletto M. thanks CNPq.

Conflicts of Interest: The authors declare no conflicts of interest.

References

1. Albertsson, A.; Karlsson, S. The Three Stages in Degradation of Polymers—Polyethylene as a Model Substance. *J. Appl. Polym. Sci.* **1988**, *35*, 1289–1302. [CrossRef]
2. Wang, Y.; Feng, G.; Lin, N.; Lan, H.; Li, Q.; Yao, D.; Tang, J. A Review of Degradation and Life Prediction of Polyethylene. *Appl. Sci.* **2023**, *13*, 3045. [CrossRef]
3. Faruk, O.; Bledzki, A.K.; Fink, H.-P.; Sain, M. Biocomposites Reinforced with Natural Fibers: 2000–2010. *Prog. Polym. Sci.* **2012**, *37*, 1552–1596. [CrossRef]
4. Geszke-Moritz, M.; Moritz, M. Biodegradable Polymeric Nanoparticle-Based Drug Delivery Systems: Comprehensive Overview, Perspectives and Challenges. *Polymers* **2024**, *16*, 2536. [CrossRef]
5. Levi, D.S.; Cheng, A.L. Biodegradable Implants. In *Pediatric and Congenital Cardiology, Cardiac Surgery and Intensive Care*; Springer: London, UK, 2014; pp. 1219–1235.
6. Kurowiak, J.; Klekiel, T.; Będziński, R. Biodegradable Polymers in Biomedical Applications: A Review—Developments, Perspectives and Future Challenges. *Int. J. Mol. Sci.* **2023**, *24*, 16952. [CrossRef]
7. Musioł, M.; Rydz, J.; Janeczek, H.; Radecka, I.; Jiang, G.; Kowalczuk, M. Forensic Engineering of Advanced Polymeric Materials Part IV: Case Study of Oxo-Biodegradable Polyethylene Commercial Bag—Aging in Biotic and Abiotic Environment. *Waste Manag.* **2017**, *64*, 20–27. [CrossRef]
8. Mastalygina, E.; Abushakhmanova, Z.; Poletto, M.; Pantyukhov, P. Biodegradation in Soil of Commercial Plastic Bags Labelled as "Biodegradable". *Mater. Res.* **2023**, *26*, e20220164. [CrossRef]
9. Mohanty, A.K.; Misra, M.; Drzal, L.T. (Eds.) *Natural Fibers, Biopolymers, and Biocomposites*; CRC Press: Boca Raton, FL, USA, 2005; ISBN 9780203508206.
10. Aleksanyan, K.V. Polysaccharides for Biodegradable Packaging Materials: Past, Present, and Future (Brief Review). *Polymers* **2023**, *15*, 451. [CrossRef]
11. Shabarin, A.A.; Kuzmin, A.M.; Matushkina, Y.I.; Shabarin, I.A. Production of Biodegradable Polymeric Packaging Materials Based on Polyolefins and Wood Flour. *Chem. Plant Raw Mater.* **2022**, 307–314. [CrossRef]
12. Sahi, S.; Djidjelli, H.; Boukerrou, A. Study of the Properties and Biodegradability of the Native and Plasticized Corn Flour-Filled Low Density Polyethylene Composites for Food Packaging Applications. *Mater. Today Proc.* **2021**, *36*, 67–73. [CrossRef]
13. Aleksanyan, K.V.; Rogovina, S.Z.; Ivanushkina, N.E. Novel Biodegradable Low-density Polyethylene–Poly(Lactic Acid)–Starch Ternary Blends. *Polym. Eng. Sci.* **2021**, *61*, 802–809. [CrossRef]
14. Foulk, J.A.; Chao, W.Y.; Akin, D.E.; Dodd, R.B.; Layton, P.A. Analysis of Flax and Cotton Fiber Fabric Blends and Recycled Polyethylene Composites. *J. Polym. Environ.* **2006**, *14*, 15–25. [CrossRef]
15. Griffin, G.J.L. Biodegradable Fillers in Thermoplastics. In *Fillers and Reinforcements for Plastics*; American Chemical Society: Washington, DC, USA, 1974; pp. 159–170, ISBN 9780841202023.
16. Padermshoke, A.; Kajiwara, T.; An, Y.; Takigawa, M.; Van Nguyen, T.; Masunaga, H.; Kobayashi, Y.; Ito, H.; Sasaki, S.; Takahara, A. Characterization of Photo-Oxidative Degradation Process of Polyolefins Containing Oxo-Biodegradable Additives. *Polymer* **2022**, *262*, 125455. [CrossRef]

17. Fa, W.; Wang, J.; Ge, S.; Chao, C. Performance of Photo-Degradation and Thermo-Degradation of Polyethylene with Photo-Catalysts and Thermo-Oxidant Additives. *Polym. Bull.* **2020**, *77*, 1417–1432. [CrossRef]
18. Chalykh, A.E.; Gerasimov, V.K.; Rusanova, S.N.; Stoyanov, O.V.; Petukhova, O.G.; Kulagina, G.S.; Pisarev, S.A. Phase Structure of Silanol-Modified Ethylene-Vinyl Acetate Copolymers. *Polym. Sci. Ser. A* **2006**, *48*, 1058–1066. [CrossRef]
19. Oluwoye, I.; Altarawneh, M.; Gore, J.; Dlugogorski, B.Z. Oxidation of Crystalline Polyethylene. *Combust. Flame* **2015**, *162*, 3681–3690. [CrossRef]
20. Jubinville, D.; Tzoganakis, C.; Mekonnen, T.H. Recycled PLA—Wood Flour Based Biocomposites: Effect of Wood Flour Surface Modification, PLA Recycling, and Maleation. *Constr. Build. Mater.* **2022**, *352*, 129026. [CrossRef]
21. Lendvai, L.; Omastova, M.; Patnaik, A.; Dogossy, G.; Singh, T. Valorization of Waste Wood Flour and Rice Husk in Poly(Lactic Acid)-Based Hybrid Biocomposites. *J. Polym. Environ.* **2023**, *31*, 541–551. [CrossRef]
22. Morreale, M.; Scaffaro, R.; Maio, A.; La Mantia, F.P. Effect of Adding Wood Flour to the Physical Properties of a Biodegradable Polymer. *Compos. Part A Appl. Sci. Manuf.* **2008**, *39*, 503–513. [CrossRef]
23. Shelenkov, P.G.; Pantyukhov, P.V.; Aleshinskaya, S.V.; Maltsev, A.A.; Abushakhmanova, Z.R.; Popov, A.A.; Saavedra-Arias, J.J.; Poletto, M. Thermal Stability of Highly Filled Cellulosic Biocomposites Based on Ethylene–Vinyl Acetate Copolymer. *Polymers* **2024**, *16*, 2103. [CrossRef]
24. Muthuraj, R.; Misra, M.; Mohanty, A.K. Biodegradable Compatibilized Polymer Blends for Packaging Applications: A Literature Review. *J. Appl. Polym. Sci.* **2018**, *135*, 45726. [CrossRef]
25. Niwa, S.; Ogawa, T.; Ogoe, S.; Teramoto, Y. Wetting and Localization of Compatibilizers in Biocomposites: A Nanoscale Evaluation and Effects on Physical Properties. *Polymer* **2019**, *185*, 121963. [CrossRef]
26. da Silveira, P.H.P.M.; dos Santos, M.C.C.; Chaves, Y.S.; Ribeiro, M.P.; Marchi, B.Z.; Monteiro, S.N.; Gomes, A.V.; de La Caridad Om Tapanes, N.; da Costa Pereira, P.S.; Bastos, D.C. Characterization of Thermo-Mechanical and Chemical Properties of Polypropylene/Hemp Fiber Biocomposites: Impact of Maleic Anhydride Compatibilizer and Fiber Content. *Polymers* **2023**, *15*, 3271. [CrossRef] [PubMed]
27. Sugumaran, V.; Kapur, G.S.; Narula, A.K. Sustainable Potato Peel Powder–LLDPE Biocomposite Preparation and Effect of Maleic Anhydride-Grafted Polyolefins on Their Properties. *Polym. Bull.* **2018**, *75*, 5513–5533. [CrossRef]
28. Li, D.; Li, J.; Hu, X.; Li, L. Effects of Ethylene Vinyl Acetate Content On Physical And Mechanical Properties of Wood-Plastic Composites. *BioResources* **2012**, *7*, 2916–2932. [CrossRef]
29. Pham, N.T.-H. Characterization of Low-Density Polyethylene and LDPE-Based/Ethylene-Vinyl Acetate with Medium Content of Vinyl Acetate. *Polymers* **2021**, *13*, 2352. [CrossRef]
30. Shelenkov, P.G.; Pantyukhov, P.V.; Popov, A.A. Highly Filled Biocomposites Based on Ethylene-Vinyl Acetate Copolymer and Wood Flour. In Proceedings of the 2018 5th Global Conference on Polymer and Composite Materials (PCM 2018), Kitakyushu City, Japan, 10–13 April 2018; 2018; Volume 369, p. 012043. [CrossRef]
31. Shelenkov, P.G.; Pantyukhov, P.V.; Popov, A.A. Mechanical Properties of Superconcentrates Based on Ethylene-Vinyl Acetate Copolymer and Microcrystalline Cellulose. *Mater. Sci. Forum* **2020**, *992*, 306–310. [CrossRef]
32. Shelenkov, P.G.; Pantyukhov, P.V.; Poletto, M.; Popov, A.A. Influence of Vinyl Acetate Content and Melt Flow Index of Ethylene-Vinyl Acetate Copolymer on Physico-Mechanical and Physico-Chemical Properties of Highly Filled Biocomposites. *Polymers* **2023**, *15*, 2639. [CrossRef]
33. Nikitin, N.I. *Chemistry of Wood and Cellulose*; Academy of Sciences of the USSR: Saint Petersburg, Russia, 1962; ISBN 978-5-458-35956-6.
34. Cavallaro, G.; Agliolo Gallitto, A.; Lisuzzo, L.; Lazzara, G. Comparative Study of Historical Woods from XIX Century by Thermogravimetry Coupled with FTIR Spectroscopy. *Cellulose* **2019**, *26*, 8853–8865. [CrossRef]
35. *ISO 527-1:2012*; Plastics—Determination of Tensile Properties: Part 1: General Principles. ISO: Geneva, Switzerland, 2012.
36. *ISO 62:2008*; Plastics—Determination of Water Absorption. ISO: Geneva, Switzerland, 2008.
37. *GOST 9.060-75*; Unified System of Protection Against Corrosion and Ageing. Fabrics. Method of Laboratory Tests for Resistance to Microbiological Destruction. State Standard of the USSR: Moscow, Russia, 1975.
38. Zykova, A.; Pantyukhov, P.; Popov, A. Mechanical Properties of Ethylene-Octene Copolymer (EOC)—Lignocellulosic Fillers Biocomposites in Dependence to Filler Content. *AIP Conf. Proc.* **2016**, *1736*, 020123. [CrossRef]
39. Mastalygina, E.E.; Abushakhmanova, Z.R.; Guyvan, M.Y.; Brovina, S.D.; Ovchinnikov, V.A.; Pantyukhov, P.V. A Study of Biodegradation Kinetics of Cellulose and Its Derivatives Using of the Sturm Test. *Russ. J. Appl. Chem.* **2022**, *95*, 1790–1799. [CrossRef]